

# On the Performance of Interference Subspace Rejection for Next Generation Multicarrier CDMA

Besma Smida and Sofïene Affes

INRS-EMT, Université du Québec  
Place Bonaventure, 800, de la Gauchetière Ouest, Suite 6900  
Montréal, Québec, H5A 1K6, Canada

**Abstract**—A multicarrier-CDMA receiver with full interference suppression capabilities, named multi-carrier interference subspace rejection (MC-ISR), has recently been proposed and assessed by simulations for high-rate transmissions over next-generation CDMA systems. In this paper, we derive a link/system-level performance analysis of MC-ISR based on the Gaussian assumption (GA) and validate it by simulations. In addition, we provide a comparative study of the two potential next-generation multicarrier CDMA air-interface configurations: MT-CDMA and MC-DS-CDMA. Simulations show that for both DBPSK and DQPSK modulations, MT-CDMA has the best link-level performance and the highest throughput. With two receiving antennas and nine MT-CDMA subcarriers in 5 MHz bandwidth, MC-ISR provides about 1.4 bps/Hz at low mobility for DBPSK, i.e., an increase of 170% in spectrum efficiency over a DS-CDMA system with MRC.

## I. INTRODUCTION

Although multi-carrier (MC)-CDMA systems are promising, challenges remain before they can achieve their full potential. One of the major obstacles in detecting MC-CDMA signals is interference. The multiple access interference (MAI) and the inter-symbol interference (ISI), which are inherited from conventional DS-CDMA, affect likewise the performance of MC-CDMA systems. In addition, MC-CDMA capacity is limited by the inter-carrier interference (ICI) due to the use of multicarrier modulation. Indeed, the imperfect frequency down-conversion due to the instability of local oscillators combined with the multipath effect disturbs the subcarriers orthogonality thereby causing ICI.

Since MC-CDMA systems also contain a DS-CDMA component, traditional multiuser detection techniques can be performed on each carrier with some form of adaptation. An efficient multiuser detection technique, denoted interference subspace rejection (ISR), first proposed for DS-CDMA [1], has been recently developed for multicarrier systems [2]. The performance of multi-carrier (MC)-ISR was evaluated there through simulations using very realistic link-level simulation setups that take into account time and frequency mismatch, imperfect power control, channel identification errors etc. Simulation results confirm the net advantage of the full interference suppression capabilities of MC-ISR.

In this paper, we develop a theoretical link/system-level performance analysis of MC-ISR based on the Gaussian assumption (GA), under the condition of perfect channel identification. In addition, we provide a comparative study of the two potential next-generation multicarrier CDMA air-interface configurations: MT-CDMA and MC-DS-CDMA.

## II. DATA MODEL AND ASSUMPTIONS

We consider the uplink of an asynchronous multi-cellular multicarrier CDMA system, with  $U$  in-cell active users, between a simple transmit antenna and  $M$  receive antennas. For the sake of simplicity, we assume that all users use the same subcarriers and transmit with the same modulation at the same rate. The input information sequence of the  $u$ -th user

is first converted into  $N_c = 2K + 1$  parallel data sequences  $b_{-K,n}^u, \dots, b_{0,n}^u, \dots, b_{K,n}^u$  where  $n$  is the time index. The data  $b_{k,n}^u \in C_{\mathcal{M}}$  is  $\mathcal{M}$ -PSK modulated and differentially<sup>1</sup> encoded at rate  $1/T_{MC}$ , where  $T_{MC} = N_c \times T$  is the symbol duration after serial/parallel (S/P) conversion and  $C_{\mathcal{M}} = \{\dots, e^{j\frac{2\pi m}{\mathcal{M}}}, \dots\}$ ,  $m \in \{0, \dots, \mathcal{M} - 1\}$ . The resulting S/P converter output is then spread with a spreading code  $c^u(t)$  at a rate  $1/T_c$ . The spreading factor, defined as the ratio between the chip rate and the symbol rate is  $L = \frac{T_{MC}}{T_c}$ . A closed-loop power control is taken into account at the transmitter. All the data are then modulated in baseband by the inverse discrete Fourier transform (IDFT) and summed to obtain the multicarrier signal. No guard interval is inserted. Indeed, the channel identification and equalization are achieved by MC-STAR (multicarrier spatio-temporal array-receiver) [3] and simulation results have shown that the guard interval length does not affect the link-level performance due to the multipath equalization capability of MC-STAR. Finally the signal is transmitted after pulse shaping and radio-frequency up-conversion. The modulated subcarriers are orthogonal over the symbol duration  $T_{MC}$ . The frequency corresponding to the  $k$ -th subcarrier is  $f_k = \lambda \times k/T_{MC}$ . The transmitter belongs to the family of MT-CDMA if  $\lambda$  is set to 1, and to the class of MC-DS-CDMA if  $\lambda$  is set to  $L$ .

The channel is assumed to be a slowly varying frequency selective Rayleigh channel with delay spread  $\Delta\tau$ . We assume correlated Rayleigh channels across subcarriers. We also assume that the received channel multipath components across the  $M$  receiving antennas are independent.

The receiver implements down conversion, matched pulse filtering and chip-rate sampling followed by framing the observation into overlapping blocks of constant length of  $N_P$  chips. Hence, we obtain the  $MN_P$  vector-shaped matched-filter observation:

$$\underline{Y}_n = \sum_{u=1}^U \sum_{k=-K}^K \sum_{n'=n-1}^{n+1} \underline{Y}_{n',k,n}^u + \underline{N}_n, \quad (1)$$

where the symbol  $n'$  of carrier  $k$  of user  $u$  contributes its vector observation  $\underline{Y}_{n',k,n}^u = s_{k,n'}^u \underline{Z}_{n',k,n}^u$ .  $\underline{Z}_{n',k,n}^u = \psi_{k,n'}^u = \psi_{k,n'}^u b_{k,n'}^u$  and  $\left(\psi_{k,n'}^u\right)^2$  are the spread channel, the  $n'$ -th signal component of the  $k$ -th carrier and the received power over carrier  $k$ , respectively. Due to asynchronism and multipath propagation, each user's observation vector carries information from current as well as from the previous and future symbols. The noise vector  $\underline{N}_n$ , which comprises the preprocessed thermal noise and the interference due to out-of-cell users, is assumed to be uncorrelated both in space and time with variance  $\sigma_N^2$ .

The total interference for user  $d$   $\underline{I}_{k,n}^d$  includes three types of interference: 1) The multiple access interference  $\underline{I}_{MAI,k,n}^d$  is due to the  $N_c$  carriers from the other in-cell users

Work supported by a Canada Research Chair in High-Speed Wireless Communications and the Strategic Grants Program of NSERC.

<sup>1</sup>We can also use pilot symbols for coherent modulation and detection [4], but that is beyond the scope of this paper.

$u \neq d$ . 2) The inter-carrier interference  $\underline{I}_{\text{ICI},k,n}^d$  is due to the other carriers,  $k' \neq k$ , from the same user  $d$ . 3) The inter-symbol interference  $\underline{I}_{\text{ISI},k,n}^d$  is due to the same carrier  $k$  from the same user  $d$ . Provided that an estimate of the total interference  $\hat{\underline{I}}_{k,n}^d = \hat{\underline{I}}_{\text{MAI},k,n}^d + \hat{\underline{I}}_{\text{ICI},k,n}^d + \hat{\underline{I}}_{\text{ISI},k,n}^d$  is made available at the receiver, we can eliminate it and yet achieve distortionless response to the desired signal by the following MC-ISR combiner:

$$\underline{W}_{k,n}^d = \frac{\mathbf{\Pi}_{k,n}^d \hat{\underline{Z}}_{n,k,n}^d}{\hat{\underline{Z}}_{n,k,n}^{dH} \mathbf{\Pi}_{k,n}^d \hat{\underline{Z}}_{n,k,n}^d}, \quad (2)$$

$$Q_n = 1 / \|\hat{\underline{I}}_{k,n}^d\|^2, \quad \mathbf{\Pi}_{k,n}^d = \mathbf{I}_{N_T} - \hat{\underline{I}}_{k,n}^d \hat{\underline{I}}_{k,n}^{dH} \times Q_n \quad (3)$$

where  $N_T = M \times N_P$  is the total space dimension and  $\mathbf{I}_{N_T}$  denotes an  $N_T \times N_T$  identity matrix. First, we form the projector  $\mathbf{\Pi}_{k,n}^d$  orthogonal to the total interference realization.

Second, we project the estimated response vector  $\hat{\underline{Z}}_{n,k,n}^d$  and normalize it to derive the MC-ISR combiner. We use this combiner to extract the  $n$ -th signal component of the  $k$ -th carrier of the desired user as:  $\hat{s}_{k,n}^d = \underline{W}_{k,n}^{dH} \underline{Y}_n$ . Unlike most of the multi-user receivers proposed for MC-CDMA which focus on multiple access interference while ignoring the inter-carrier-interference, MC-ISR fully suppresses the total interference resulting from MAI, ISI, and ICI by simple yet efficient nulling.

### III. PERFORMANCE ANALYSIS OF MC-ISR

This section is dedicated to the performance analysis of the MC-ISR receiver based on the Gaussian assumption (GA). We exploit the analysis results of DS-CDMA ISR recently developed in [5] at the link-level and extend them to MC-ISR. Additionally, we broaden the scope of the analysis to the system level.

#### A. Link-Level Performance

For the sake of simplicity, we assume temporarily perfect channel identification. Later in the simulations, we will use the channel and CFO estimates provided by MC-STAR<sup>2</sup> [3]. The post-combined signal can be formulated as:

$$\hat{s}_{k,n}^d = \underline{W}_{k,n}^{dH} \underline{Y}_n = s_{k,n}^d + \delta_{\text{MAI}}^{d,k,n} + \delta_{\text{ICI}}^{d,k,n} + \delta_{\text{ISI}}^{d,k,n} + \underline{W}_{k,n}^{dH} \underline{N}_n, \quad (4)$$

where  $\delta_{\text{MAI}}^{d,k,n}$  is the residual MAI,  $\delta_{\text{ICI}}^{d,k,n}$  is the residual ICI, and  $\delta_{\text{ISI}}^{d,k,n}$  is the residual ISI. We assume here that the interference rejection residuals  $\delta_{\text{MAI}}^{d,k,n}$ ,  $\delta_{\text{ICI}}^{d,k,n}$ , and  $\delta_{\text{ISI}}^{d,k,n}$  are Gaussian random variables with zero mean. Hence, we only need to evaluate their variances. Note that the residuals would be null (i.e.,  $\delta_{\text{MAI}}^{d,k,n} = \delta_{\text{ICI}}^{d,k,n} = \delta_{\text{ISI}}^{d,k,n} = 0$ ) if the reconstruction of the interference were perfect (i.e.,  $\hat{\underline{I}}_{k,n}^d = \underline{I}_{k,n}^d$ ) and hence  $\hat{s}_{k,n}^d = s_{k,n}^d + \underline{W}_{k,n}^{dH} \underline{N}_n$  would be corrupted only by the residual noise, which is Gaussian with zero mean and variance:

$$\text{Var}[\underline{W}_{k,n}^{dH} \underline{N}_n] = \bar{\kappa} \sigma_N^2, \quad (5)$$

where  $\bar{\kappa} = E[\|\underline{W}_{k,n}^d\|^2] = \frac{ML-1}{ML-2}$ , is a measure of the enhancement of the white noise compared to MRC ( $\bar{\kappa} = 1$  for MRC) [5]. However, in practice the interference vector is reconstructed erroneously due to wrong tentative data decisions and  $\hat{s}_{k,n}^d$  is further corrupted by non-null residual interference rejection components. Hence, we introduce the

<sup>2</sup>Simulations will show little deviation from analysis in the operating BER region.

error indicating variable  $\xi_{k,n}^d = b_{k,n}^d * \hat{b}_{k,n}^d$ , where  $(\cdot)^*$  means complex conjugate.  $\xi_{k,n}^d$  equals 1 when the estimated data symbol is correct; otherwise it is a complex number. The signal after MC-ISR combining is then:

$$\begin{aligned} \underline{W}_{k,n}^{dH} \underline{Y}_n &= s_{k,n}^d + \sum_{u \neq d}^U \sum_{k'=-K}^K \sum_{n'=n-1}^{n+1} \xi_{n',k}^u \underline{W}_{k,n}^{dH} \hat{\underline{Y}}_{n',k',n}^u \\ &+ \sum_{k' \neq k}^K \sum_{n'=n-1}^{n+1} \xi_{n',k'}^d \underline{W}_{k,n}^{dH} \hat{\underline{Y}}_{n',k',n}^d \\ &+ \sum_{n'=n-1}^{n+1} \sum_{n' \neq n} \xi_{n',k}^d \underline{W}_{k,n}^{dH} \hat{\underline{Y}}_{n',k,n}^d + \underline{W}_{k,n}^{dH} \underline{N}_n. \end{aligned} \quad (6)$$

The MC-ISR combiner  $\underline{W}_{k,n}^d$  satisfies the optimization property in Eq. (2), thus

$$\text{Var}[\underline{W}_{k,n}^{dH} (\hat{\underline{I}}_{\text{MAI},k,n}^d + \hat{\underline{I}}_{\text{ICI},k,n}^d + \hat{\underline{I}}_{\text{ISI},k,n}^d)] = 0. \quad (7)$$

This result allows to derive the variance of the interference rejection residuals. The interferences  $\underline{I}_{k,n}^d$  are approximated as a Gaussian distributed random variable with zero mean. Only their variance needs to be evaluated. We suppose that  $E[\|\underline{W}_{k,n}^d\|^2] = \bar{\kappa}$ , which is a measure of the enhancement of the white noise compared to MRC combiner [5]. We also assume that the combiner  $\underline{W}_{k,n}^d$  and  $\hat{\underline{Y}}_{n',k',n}^u$  are uncorrelated. Let  $\bar{\psi}_D^2 = E[(\psi_k^d)^2]$  be the average power of the  $k$ -th carrier of the desired user and  $\bar{\psi}_I^2$  be the average interference power on each interfering carrier (assumed equal for all  $u$  and all  $k$ ). The variances of the residual interferences can be written as:

$$\begin{aligned} \text{Var}[\delta_{\text{MAI}}^{d,k,n}] &= \bar{\psi}_I^2 (U-1) \left[ \frac{1}{L} + \text{Sum} \right] (1 - \rho_\xi) \bar{\kappa}, \\ \text{Var}[\delta_{\text{ICI}}^{d,k,n}] &= \delta_{is} \bar{\psi}_D^2 [\text{Sum}] (1 - \rho_\xi) \bar{\kappa}, \\ \text{Var}[\delta_{\text{ISI}}^{d,k,n}] &= \bar{\psi}_D^2 (1 - \rho_\xi) (\bar{\kappa} - 1 + \delta_{is}) / L, \\ \text{Sum} &= \sum_{k' \neq k}^K \frac{L}{\pi^2 (k'-k)^2 \lambda^2} (1 - \text{sinc}(\frac{2\pi(k'-k)\lambda}{L})), \end{aligned} \quad (8)$$

where  $\rho_\xi = E[\xi_{k,n}^u \xi_{k',n}^u]$  and  $\delta_{is}$  ( $0 \leq \delta_{is} < 1$ ) is a measure of the relative impact of the interference generated by the other paths on a given path of the desired user [5]. In the developments of Eq. (8) above, we exploited the expression for the variance of the interference derived in [6]. However, we introduced a correction factor of 3/2 to the variance of the MAI interference due to the same carrier because we consider practical square-root raised cosine pulses [7][8]. Notice also that since we transmit different data sequences over distinct subcarriers for a given user, the cross-correlation terms from different subcarriers are uncorrelated. Hence, there is no effect of the correlation between subcarriers on the amount of residual interference in MC-CDMA systems with the MC-ISR receiver. The SNR on the  $k$ -th carrier can be estimated as:

$$\text{SNR}_{\text{ISR}}^k = \frac{M \bar{\psi}_D^2}{\text{Var}[\delta_{\text{MAI}}^{d,k,n}] + \text{Var}[\delta_{\text{ICI}}^{d,k,n}] + \text{Var}[\delta_{\text{ISI}}^{d,k,n}] + \bar{\kappa} \sigma_N^2}. \quad (9)$$

The average signal to noise ratio  $\text{SNR}_{\text{ISR}}$  is given by  $\frac{1}{2K+1} \sum_{k=-K}^K \text{SNR}_{\text{ISR}}^k$ . Note that the SNR expression above applies to MRC as well by setting  $\bar{\kappa} = 1$  and  $\rho_\xi = 0$  in Eq. (8). The BER performance of the MC-ISR receiver is then given as follows:

$$P_e = \Omega(\text{SNR}_{\text{ISR}}), \quad (10)$$

where  $\Omega$  represents the single user bound (SUB), which is classically defined as a conditional Gaussian Q-function over  $\psi_D$  and  $\psi_I$ . When using this classical representation, the average BER is derived by first finding the pdfs of  $\psi_D$  and  $\psi_I$  and then averaging over those pdfs. Since it is difficult to

find a simple expression for the pdfs of  $\psi_D$  and  $\psi_I$ , we may consider an approximative pdf. In this analysis, we choose to simulate  $\Omega$  without imposing any pdf approximation. The simulations will later consider a realistic wireless channel with imperfect power control and imperfect channel identification.

### B. System-Level Performance

In order to compare the different MC-ISR configurations, the link-level curves provide a good picture of the performance of each system. But limiting comparisons to the BER performance is not sufficient because the data rate is not equal for all configurations. Hence, we translate the link-level results into system-level results in terms of total throughput (or spectrum efficiency) under the following three assumptions: 1) All users are received with an equal average power (i.e.,  $\overline{\psi}_D^2 = \overline{\psi}_I^2$ ). 2) All the cells have the same load of  $C$  users per cell. 3) The out-cell to in-cell interference ratio  $f$  is set to 0.6. Given these assumptions in an interference-limited system (noise is low compared to interference), the link-level required SNR at the base-station antennas (ignoring ISI for simplicity) is:

$$SNR_{req} = \frac{1}{\delta_{is}(1 - \rho_\xi)\overline{\kappa}\beta + (C - 1)\alpha + Cf\gamma}, \quad (11)$$

where

$$\begin{aligned} \beta &= \text{mean}_k \left[ \sum_{\substack{k'=-K \\ k' \neq k}}^K \frac{L}{\pi^2(k'-k)^2\lambda^2} (1 - \text{sinc}(\frac{2\pi(k'-k)\lambda}{L})) \right], \\ \alpha &= (\frac{1}{L} + \beta)(1 - \rho_\xi)\overline{\kappa}, \\ \gamma &= (\frac{1}{L} + \beta). \end{aligned} \quad (12)$$

The maximum number of users that can access the system can be hence calculated as:

$$C_{max} = \lfloor (\frac{1}{SNR_{req}} - \delta_{is}(1 - \rho_\xi)\overline{\kappa}\beta + \alpha)(\frac{1}{\alpha + \gamma f}) \rfloor, \quad (13)$$

where  $\lfloor \cdot \rfloor$  is the floor function. The total throughput is hence  $\mathcal{T}_{max} = C_{max} \times R_b = C_{max} \times R_s \times \log_2(\mathcal{M})$ , where  $R_b$  and  $R_s$  are the bit rate and the symbol rate over all subcarriers, respectively. We also define the spectrum efficiency as  $\mathcal{E}_{max} = \mathcal{T}_{max}/BW$ .

## IV. SIMULATION RESULTS

### A. Simulation Setup

We consider an MC-CDMA system operating at a carrier of 1.9 GHz with maximum bandwidth of 5 MHz. We select a frequency offset  $\Delta f$  of 200 Hz, the maximum error tolerated by 3G standards ( $\equiv 0.1$  ppm) for the frequency mismatch between the mobile and the base station [9]. We assume a frequency selective Rayleigh fading channel with  $P$  propagation paths with exponentially decreasing powers. The channel is correlated across subcarriers and varying in time with Doppler shift  $f_D$ . We consider that time-delays vary linearly in time with a delay drift of 0.049 ppm. The receiver has  $M = 1$  or 2 antennas. We implement closed-loop power control operating at 1600 Hz and adjusting the power in steps of  $\pm 0.25$  dB. An error rate on the power control bit of 5% and a feedback delay of 0.625 ms are simulated. Table I shows the parameters specific to each multicarrier CDMA configuration. We choose as a reference the 3G DS-SS-CDMA ( $N_c = 1$ ) system with spreading factor  $L = 32$  and chip rate of 3.84 Mcps. We assume frequency selective fading with  $P = 3$  propagation paths. One of the features of MT-CDMA is that for a constant bandwidth the ratio between the spreading factor  $L$  and  $2K = N_c - 1$  is constant. We hence maintain the same chip rate (3.840 Mcps) by changing the spreading factor and the number of subcarriers. We consider four MT-CDMA configurations.

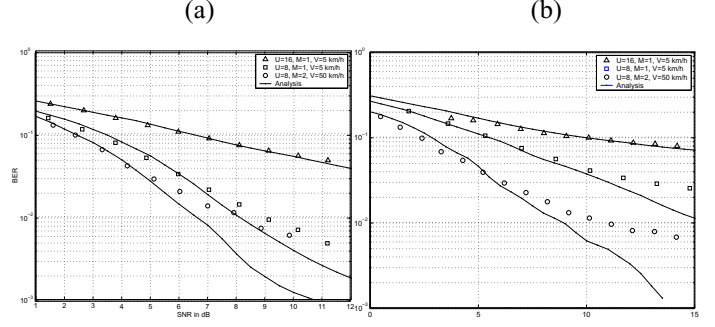


Fig. 1. Analytical and simulated BER vs. SNR in dB for (a): MT-CDMA,  $L = 64$ ,  $N_c = 3$ , DBPSK and (b): MC-DS-CDMA  $L = 32$ ,  $N_c = 3$ , DBPSK.

Since they use the same chip rate, there are three paths in each MT-CDMA subcarrier. For a fair comparison among different configurations of MC-DS-CDMA, the bandwidth should be the same. By reducing the chip rate, we varied the number of subcarriers while maintaining the orthogonality between them. Due to the reduction in bandwidth, each subcarrier in MC-DS-CDMA has either two paths (i.e.,  $P = 2$ ) or one path (i.e.,  $P = 1$ , frequency nonselective fading) for  $N_c = 3$  and  $N_c \geq 5$ , respectively. The main performance criterion is the link-level SNR required per carrier to meet a BER of 5% in order to achieve a QoS of  $10^{-6}$  after channel decoding and the resulting system-level spectrum efficiency. The user's data rate is calculated by adding the data rates over all subcarriers.

### B. Validation of the Performance Analysis

In this section, we investigate the accuracy of the analytical performance analysis in section III under realistic channel conditions. Indeed we do not assume perfect channel identification; instead we use the channel estimate provided by MC-STAR [3]. We validate the Gaussian approximation (GA) of the interference by comparison with simulation results. Since the SUB ( $\Omega$ ) is not known explicitly in this case, it has been obtained from extensive simulations. We consider two configurations: DBPSK MT-CDMA ( $L = 64$ ,  $N_c = 3$ ); and DBPSK MC-DS-CDMA ( $L = 32$ ,  $N_c = 3$ ). Fig. 1 shows the link-level performance. It is seen, not surprisingly, that the GA is accurate in the presence of moderate background noise. The precision of GA increases with the number of users and at a low-Doppler situation. In the target BER (5%) region, despite the realistic channel model employed, there is a good match between analytical and simulation results for both MT-CDMA and MC-DS-CDMA. This suggests that the analytical evaluation is accurate in a low-Doppler situation.

### C. MT-CDMA, MC-DS-CDMA, and DS-CDMA Performance Comparison

This section is dedicated to the performance comparison of the proposed MC-ISR receiver with two potential next-generation multicarrier CDMA air-interface configurations: MT-CDMA and MC-DS-CDMA. Single-carrier MRC over current 3G DS-SS-CDMA is also considered as a reference. First, we derive the  $SNR_{req}$  from link-level simulations. Then, we translate the link-level results into system-level results using Eq. (13). In Table II, we provide the required SNR and the total throughput of DBPSK and D8PSK modulated data with two receiving antennas ( $M = 2$ ) for DS-SS-CDMA, MT-CDMA, and MC-DS-CDMA. For DBPSK modulation, we observe that we can improve the system performance by increasing the number of subcarriers. Indeed, the required SNR continues to decrease despite the increase in the number of carriers, due to ICI suppression. Table II also shows that MT-CDMA outperforms MC-DS-CDMA with DBPSK modulation

Parameter	DS-CDMA	MT-CDMA				MC-DS-CDMA				Comment
$\lambda$	-	1				$L$				subcarrier spacing parameter
$N_c$	1	3	5	7	9	3	5	7	9	number of subcarriers
$L$	32	64	128	192	256	32	32	32	32	spreading factor
$R_c$ in Mcps	3.840	3.840				1.920	1.280	0.960	0.768	chip rate
$P$	3	3				2	1	1	1	number of paths per subcarrier
$R_s$ in kbaud	120	180	150	140	135	180	200	210	216	symbol rate over all subcarriers
$R_b$ for DBPSK in kbps	120	180	150	140	135	180	200	210	216	peak rate for DBPSK
$R_b$ for D8PSK in kbps	360	540	450	420	405	540	600	630	648	peak rate for D8PSK
$BW_{nor}$	1	1.016				1				bandwidth normalized vs. DS-CDMA

TABLE I  
PARAMETERS OF EACH MULTICARRIER SYSTEM CONFIGURATION.

MC-STAR configuration	DS-CDMA	MT-CDMA				MC-DS-CDMA			
$N_c$	1	3	5	7	9	3	5	7	9
Modulation	DBPSK								
$SNR_{req}$ in dB	0.76	0.76	0.5	0.44	<b>0.12</b>	2.87	2.26	2.26	1.77
$C_{max}$	17	25	33	37	<b>41</b>	15	15	15	16
$T_{max}$ in kbps	2040	4500	4950	5180	<b>5535</b>	2700	3000	3150	3456
$\mathcal{E}_{max}$ in bps/Hz	0.5313	1.1719	1.2891	1.3490	<b>1.4414</b>	0.7031	0.7813	0.8203	0.9000
Modulation	D8PSK								
$SNR_{req}$ in dB	8.57	<b>7.86</b>	8.89	9.57	10.55	10.01	9.6	9.53	9.12
$C_{max}$	3	<b>4</b>	4	4	3	3	3	3	3
$T_{max}$ in kbps	1080	<b>2160</b>	1800	1680	1215	1620	1800	1890	1944
$\mathcal{E}_{max}$ in bps/Hz	0.2813	<b>0.5625</b>	0.4688	0.4375	0.3164	0.4219	0.4688	0.4922	0.5062

TABLE II

REQUIRED SNR, CAPACITY, MAXIMUM THROUGHPUT, AND SPECTRAL-EFFICIENCY OF DS-CDMA (WITH MRC) AND MT-CDMA AND MC-DS-CDMA (WITH MC-ISR AND FULL INTERFERENCE SUPPRESSION) FOR DBPSK AND D8PSK (BEST PERFORMANCE VALUES FOR EACH MODULATION ARE IN BOLD).

because it uses longer spreading sequences and it exploits the subcarrier correlation. Moreover, due to the reduced subcarrier bandwidth, MC-DS-CDMA has less frequency diversity, while MT-CDMA is better able to exploit path diversity and hence achieves better performance. Note also that MC-DS-CDMA is more robust against ICI, but in applying MC-ISR, this advantage over MT-CDMA becomes obsolete.

Next, we compare different configurations with D8PSK modulation. We notice a link-level deterioration for MT-CDMA as the number of subcarriers increases. Indeed, higher-order modulation is more sensitive to the residual ICI. MC-DS-CDMA is much less affected by this phenomenon because it is much more robust to ICI thanks to the higher subcarrier spacing. Therefore, with high-order modulation MC-DS-CDMA outperforms MT-CDMA when the number of subcarriers is high enough. It is clear, however, that D8PSK is less spectrum-efficient than DBPSK modulation for all MC-ISR air-interface configurations.

In Table II we highlight the most spectrum-efficient MC-ISR air-interface configuration for each modulation. For both modulations MT-CDMA has the best link-level performance and the highest throughput (for a tested number of carriers less or equal to 9). MT-CDMA with nine subcarriers and DBPSK modulation outperforms all other configurations and provides a spectrum efficiency about 170% higher than that achievable with single-carrier MRC over a 3G DS-CDMA air-interface. In order to provide a more detailed picture of the aggregate gain of the proposed MC-ISR receiver over a potential next-generation MT-CDMA system with DBPSK modulation, we also compared its performance vs. MC-MRC over the same MT-CDMA air-interface, and vs. single-carrier ISR [1] over a 3G DS-CDMA air-interface. The corresponding spectrum efficiency gains of about 70 and 50% reported underline, respectively, the net benefits due to the proposed MC-ISR combiner and to the potential migration to a next-generation MT-CDMA air-interface.

## V. CONCLUSIONS

In this contribution, we derived a link/system-level performance analysis of MC-ISR based on the Gaussian assumption (GA), under the condition of perfect channel identification. In

addition, we provided a comparative study of the two potential next-generation multicarrier CDMA air-interface configurations: MT-CDMA and MC-DS-CDMA. Simulation results support the validity of the analysis under practical conditions. The gains in spectrum efficiencies attainable by MC-ISR are significant and are evaluated for MT-CDMA and MC-DS-CDMA as a function of the number of subcarriers and modulation. For both DBPSK and DQPSK modulations, MT-CDMA has the best link-level performance and the highest throughput. With two receiving antennas and nine MT-CDMA subcarriers in 5 MHz bandwidth, MC-ISR provides about 1.4 bps/Hz at low mobility for DBPSK, i.e., an increase of 170% in spectrum efficiency over a DS-CDMA system with MRC.

## REFERENCES

- [1] S. Affes, H. Hansen, and P. Mermelstein, "Interference subspace rejection: a framework for multiuser detection in wideband CDMA", *IEEE J. Select. Areas in Comm.*, vol. 20, no. 2, pp. 287-302, Feb. 2002.
- [2] B. Smida, S. Affes, K. Jamaoui, and P. Mermelstein, "A Multicarrier-CDMA Receiver with Full Interference Suppression and Carrier Frequency Offset Recovery", *Proc. of IEEE Signal Processing Workshop on Signal Processing Advances in Wireless Communications SPAWC'05*, New York City, New York, USA, to appear, June 6-8, 2005.
- [3] B. Smida, S. Affes, J. Li, and P. Mermelstein, "Multicarrier-CDMA STAR with time and frequency synchronization", in *Proc. IEEE ICC 2005*, to appear.
- [4] S. Affes and P. Mermelstein, "Adaptive space-time processing for wireless CDMA", *Book Chapter, Adaptive Signal Processing: Application to Real-World Problems*, J. Benesty and A.H. Huang, Eds., Springer, Berlin, January 2003.
- [5] H. Hansen, S. Affes, and P. Mermelstein, "Performance analysis of interference subspace rejection", submitted to *IEEE Trans. on Communications*, under review.
- [6] Y. Lie-Liang and L. Hanzo, "Performance of generalized multicarrier DS-CDMA over Nakagami-m fading channels", *IEEE Transactions on Communications*, vol. 50, no. 6, pp. 956-966, June 2002.
- [7] K. Cheikhrouhou, S. Affes, and P. Mermelstein, "Impact of synchronization on performance of enhanced array-receivers in wideband CDMA networks", *IEEE J. Select. Areas in Commun.*, vol. 19, no 12, pp. 2462-2476, December 2001.
- [8] Y. Asano, Y. Daido, and J. Holtzman, "Performance evaluation for band-limited DS-CDMA communication system", *IEEE VTC 1993*, pp. 464 - 468.
- [9] 3GPP TS 25.101 V5.4.0, 3rd Generation Partnership Project (3GPP), Technical Specification Group (TSG), Radio Access Network (RAN), UE Radio Transmission and Reception (FDD), September 2002.